Article

Peptide−Membrane Binding: Effects of the Amino Acid Sequence

Yanxing Yang and Cristiano L. Dias*

Read Online

ACCESS | Metrics & More | Article Recommendations | SI Supporting Information

ABSTRACT: An understanding of how the amino acid sequence affects the interaction of peptides with lipid membranes remains mostly unknown. This type of knowledge is required to rationalize membrane-induced toxicity of amyloid peptides and to design peptides that can interact with lipid bilayers. Here, we perform a systematic study of how variations in the sequence of the amphipathic Ac-(FKFE)$_2$-NH$_2$ peptide affect its interaction with zwitterionic lipid bilayers using extensive all-atom molecular dynamics simulations in explicit solvent. Our results show that peptides with a net positive charge bind more frequently to the lipid bilayer than neutral or negatively charged sequences. Moreover, neutral amphipathic peptides made with the same numbers of phenylalanine (F), lysine (K), and glutamic (E) amino

acids at different positions in the sequence differ significantly in their frequency of binding to the membrane. We find that peptides bind with a higher frequency to the membrane if their positive lysine side chains are more exposed to the solvent, which occurs if they are located at the extremity (as opposed to the middle) of the sequence. Non-polar residues play an important role in accounting for the adsorption of peptides onto the membrane. In particular, peptides made with less hydrophobic non-polar residues (e.g., valine and alanine) are significantly less adsorbed to the membrane compared to peptides made with phenylalanine. We also find that sequences where phenylalanine residues are located at the extremities of the peptide have a higher tendency to be adsorbed.
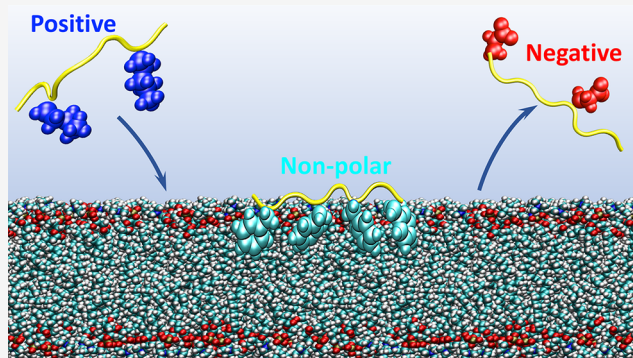
INTRODUCTION

The interaction of amphipathic peptides with lipid membranes is related to the toxicity of amyloid proteins,[1−3] the antimicrobial properties of certain peptides,[4−6] and the ability of cell penetrating peptides (CPP) to be used in several biomedical applications including drug delivery systems.[7,8] These peptides are made of polar residues that interact electrostatically with lipid head groups and non-polar side chains that become buried inside the dry membrane core via hydrophobic effects.[9−11] Currently, it remains unknown how the position of charged and non-polar residues in the sequence affects the interaction of a peptide with the membrane. This type of knowledge is critical to optimize the design of peptides as well as to rationalize the broad scope of sequences known to interact with lipid membranes.

The interaction of peptides with lipid membranes is often studied in experiments where peptides damage vesicles in solutions.[12−17] These studies are performed by comparing leakage of vesicles varying in their lipid composition as well as by using different peptides in the presence and absence of cations in solution. Membranes with a higher content of anionic lipids are found to promote both amyloid aggregation into fibrils and membrane damage.[18−20] This highlights the importance of electrostatic interactions in attracting peptides to the vicinity of negatively charged lipids promoting the formation of amyloid fibrils.[21−24] Accordingly, most CPP and

antimicrobial peptides are made of positive sequences with a net charge greater than +2. Moreover, increasing the net charge of these sequences using point mutations increases the antimicrobial activity of these peptides.[21,22] Consistent with these studies, divalent cations (e.g., calcium) are attracted and adsorbed onto lipid membranes.[9,20,25,26] This causes positive moieties of peptides to be repelled from the positive lipid−calcium complex,[9,27] which accounts for a significant reduction in pore formation on the membrane surface by amyloid peptides.[28−30] Also, the ability of antimicrobial peptides to damage red blood cells (i.e., hemolysis) was shown to depend on the position of positively charged residues in the sequence,[23] implying that the sequence pattern can be as important as the net charge in accounting for peptide−membrane interactions. In addition to electrostatic interactions, a certain degree of hydrophobicity is also required to enable the adsorption of peptides onto the membrane surface.[23,31−37] However, increasing and decreasing the hydrophobicity of antimicrobial peptides beyond a given
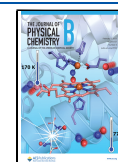
window was shown to reduce the ability of these peptides to damage lipid membranes.

Despite the important insights obtained from studies of membrane damage, it is important to highlight that the latter is affected not only by how peptides interact with lipid bilayers but also by how they interact with each other in the vicinity of membranes causing damage. Decoupling these effects is important to design sequences with specific function, e.g., as probes for organelles (e.g., mitochondria) that need to interact with the lipid membrane without causing damage.[38] Computer simulations can be used to study peptide–membrane interactions independently of how peptides damage the membrane.

Here, we perform a systematic study of the interaction of peptides with zwitterionic lipid membranes using all-atom molecular dynamics simulations. In particular, we investigate the effects of the net charge, hydrophobicity, and sequence pattern of the peptide. We find that adding positive and negative residues to the amphipathic Ac-(FKFE)-NH$_2$ peptide increases and decreases, respectively, its affinity to the membrane. Moreover, the frequency with which a peptide encounters the membrane is also affected by the position of its positive residues in the peptide sequence. The latter affects the extent by which positive side chains are exposed to the solvent and, thus, can be attracted to the membrane. We find that positive residues located close to both extremities of a peptide (i.e., C- and N-terminals) are more exposed to the solvent and, thus, encounter the membrane with a higher frequency. Peptide adsorption involves burying non-polar residues into the dry core of the lipid bilayer. Accordingly, we find that amphipathic peptides made using non-polar residues that are highly hydrophobic (i.e., phenylalanine) are adsorbed in all our simulations as opposed to peptides made using alanine and valine. In the same vein, we observe that the position of non-polar residues in the peptide sequence affects its tendency to be adsorbed into the membrane. Sequences with phenylalanine at the extremity of the peptide sequence have a higher tendency to be adsorbed in our simulations.

■ METHODOLOGY

To study peptide–membrane binding, we use an amphipathic peptide wherein non-polar (i.e., phenylalanine **F**) and charged (i.e., positive lysine **K** and negative glutamic acid **E**) residues alternate along the sequence, i.e., Ac-(**FKFE**)$_2$-NH$_2$—see Figure 1a. This *reference* peptide was shown to self-assemble into amyloid-like fibril structures in both computer simulations and experiments.[39−41] Moreover, in all-atom simulations, it was shown to bind to lipid membranes in less than 1 μs, making it suitable for computational studies.[9] We study membrane binding of 15 peptides made by adding positive (K) or negative (E) amino acids to the N-terminus of the reference sequence or by scrambling the position of its residues. A comparative study of membrane binding by these peptides allowed us to provide insights into the effects of net charge and position of charged residues on the peptide sequence. Membrane binding was also studied for peptides where phenylalanine residues of the reference peptide were replaced with valine or alanine to provide insights into effects of non-polar side chains. A list of peptides simulated in this study is provided in Table 1.

A zwitterionic bilayer made with 64 phosphatidylcholine (POPC) lipids in each leaflet is used to study membrane binding—see Figure 1b. This membrane was created using
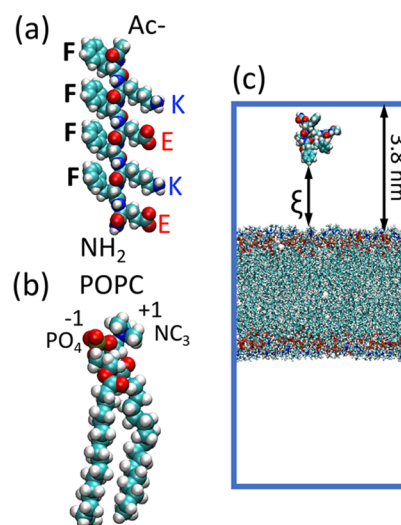

Figure 1. Atomic representation of (a) the reference peptide and (b) a POPC lipid. (c) Schematic representation of the simulation box and the minimum distance ξ between the peptide and the lipid bilayer.

Table 1. List of Sequences Simulated in This Study[a]

Sequence	Traj.	Time
Ac-(FKFE)$_2$-NH$_2$	7	5 μs
Ac-K$_2$(FKFE)$_2$-NH$_2$	5	5 μs
Ac-K$_4$(FKFE)$_2$-NH$_2$	8	8 μs
Ac-E$_2$(FKFE)$_2$-NH$_2$	5	5 μs
Ac-E$_4$(FKFE)$_2$-NH$_2$	5	5 μs
Ac-KFFEEFFK-NH$_2$	5	5 μs
Ac-KEF$_4$KE-NH$_2$	5	5 μs
Ac-(KFFE)$_2$-NH$_2$	5	5 μs
Ac-FEFKFKFE-NH$_2$	5	5 μs
Ac-KKF$_4$EE-NH$_2$	5	5 μs
Ac-FKKFFFEE-NH$_2$	5	5 μs
Ac-EFFKKFFE-NH$_2$	5	5 μs
Ac-FFKKFFEE-NH$_2$	5	5 μs
Ac-(VKVE)$_2$-NH$_2$	7	5 μs
Ac-(AKAE)$_2$-NH$_2$	5	5 μs

[a]The number of different trajectories for each sequence and the total simulated time are provided in columns 2 and 3.

CHARMM-GUI[42−44] in a box of initial size 6.6 × 6.6 × 12 nm³. For each of the 15 peptides studied here, five to eight simulations were performed by adding the peptide randomly to the simulation box at a distance larger than 2 nm from the membrane. The system was solvated with TIP3P water molecules. In the case of charged peptides, sodium/chloride ions were added to the solution to account for systems with zero charge. These monovalent ions do not interact strongly with lipids and peptide,[25,26] and thus, their presence does not significantly affect peptide–membrane binding when compared to divalent ions,[9] e.g., Ca²⁺. Figure 1c shows a typical simulation box without water molecules and the minimal distance ξ between atoms of the peptide and the membrane, which is one of the main quantities computed in this study.

All the systems were equilibrated using the two sets of three 5 ps simulations provided by CHARMM-GUI. In the first set, simulations were performed in the *NVT* ensemble with the magnitude of atomic restraints reduced after each simulation. The second set of simulations were performed in a similar fashion in the *NPT* ensemble.
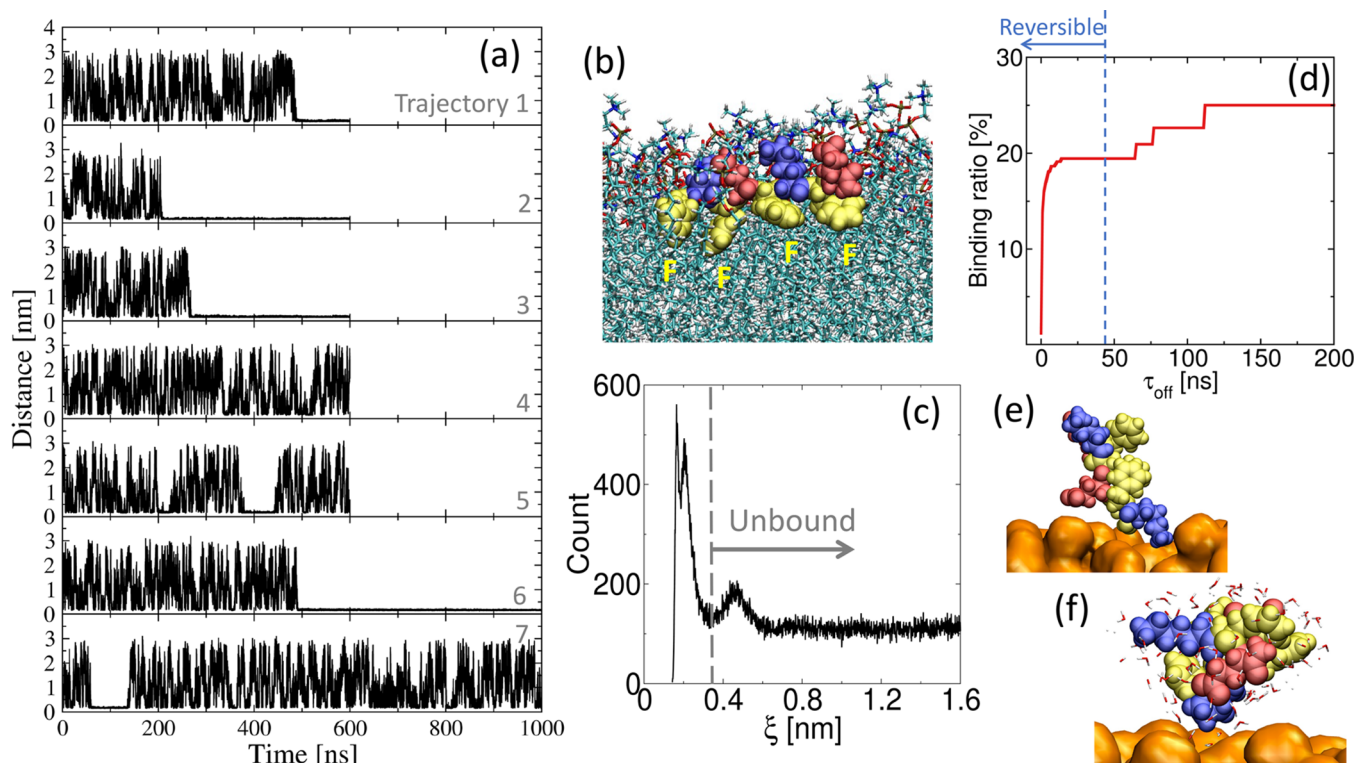
Figure 2. (a) The minimum distance ξ between atoms of the reference peptide and the lipid bilayer in seven independent simulations. (b) schematic representation of adsorbed peptide on the membrane with non-polar residues (**F**) in yellow, positive ones (K) in blue, and negative ones (E) in red. (c) distribution of ξ computed from all the reversible trajectories of the reference peptide. ξ_{cutoff} is highlighted by a gray vertical dashed line. (d) dependence of the binding ratio on τ_{off}. Characteristic conformations of binding frames with peptide in (e) direct contact and (f) solvated.

Simulations were performed using GROMACS-2020[45] with the CHARMM36m force field.[46] Equations of motion were integrated using the leapfrog algorithm with a 2 fs time step. The Nóse−Hoover thermostat (310 K and $\tau_T = 1$ ps)[47,48] and the Parrinello−Rahman barostat (1 bar and $\tau_p = 5$ ps)[49] were used to perform simulations in the NPT ensemble. A Verlet-list was used to account for first-neighbors, wherein the cutoff for van der Waals interactions was set to be 1.2 nm. The smooth particle mesh Ewald scheme with a grid spacing of 0.12 nm and a real space cutoff of 1.2 nm was used to treat electrostatic interactions.[50]

■ RESULTS AND DISCUSSION

Peptide−Membrane Simulations. Figure 2a shows the distance ξ between atoms of the peptide and the bilayer in the seven simulations performed using the reference peptide. In these trajectories, the peptide experiences several binding and unbinding events as ξ increases and decreases. In four simulations (labeled 1, 2, 3, and 6), the peptide becomes adsorbed onto the membrane surface after several hundreds of nanoseconds. In the adsorbed state, non-polar side chains are buried into the dry core of the bilayer and charged residues are exposed to the solvent—see panel b. In the time frame of our simulations, the reference peptide does not get desorbed.

One of the goals of this study is to provide insights into the attraction of peptides to the membrane. Thus, a main focus is on the reversible binding−unbinding events that take place before the peptide gets adsorbed. Since lifetimes of adsorbed and "reversible" bound states are very different, we distinguish between these states by tracking the the residence time (or binding-time) of every binding event in which the peptide

encounters the membrane. If this time is longer than a cutoff time τ_{off}, we consider the peptide to be adsorbed. Portions of the trajectory in which the peptide is adsorbed are not taken into account in the analysis. Figure 2c shows the distribution of ξ computed from all the reversible trajectories of the reference peptide using $\tau_{off} = 45$ ns. This distribution is characterized by three peaks at positions 0.17, 0.21, and 0.47 nm. In the first two peaks, the peptide is in direct contact with the bilayer (see panel e), whereas it remains solvated in the third broad peak— see panel f. Accordingly, we use the minimum between the second and third peaks, i.e., $\xi_{cutoff} = 0.325$ nm, as a cutoff to define bound states of the peptide.

A main quantity computed in this study is the fraction of all reversible frames in which the peptide is found bound to the membrane. This quantity is referred to as the "binding ratio" of the peptide. The dependence of the latter on τ_{off} is shown in Figure 2d. Initially, the binding ratio increases abruptly and it saturates at $\tau_{off} \sim 20$ ns. For larger values of τ_{off}, the binding ratio increases in small steps highlighting the existence of only a small number of binding events that survive for a long time, i.e., adsorbed states. The comparison of the binding ratio for the different peptides studied in this work does not depend on the actual choice of τ_{off} except for two sequences—see Figures S16 and S17. The latter cases involve a single event where the peptide remains bound to the membrane for more than 60 ns before detaching from it. Since our simulations are not long enough to sample these rare long binding events, binding ratios are computed using $\tau_{off} = 45$ ns. For all the simulated peptides in this study, the dependence of the "binding ratio" on τ_{off} is reported in the Supporting Information—see Figures S16 and S17. Error bars correspond to statistical uncertainties estimated
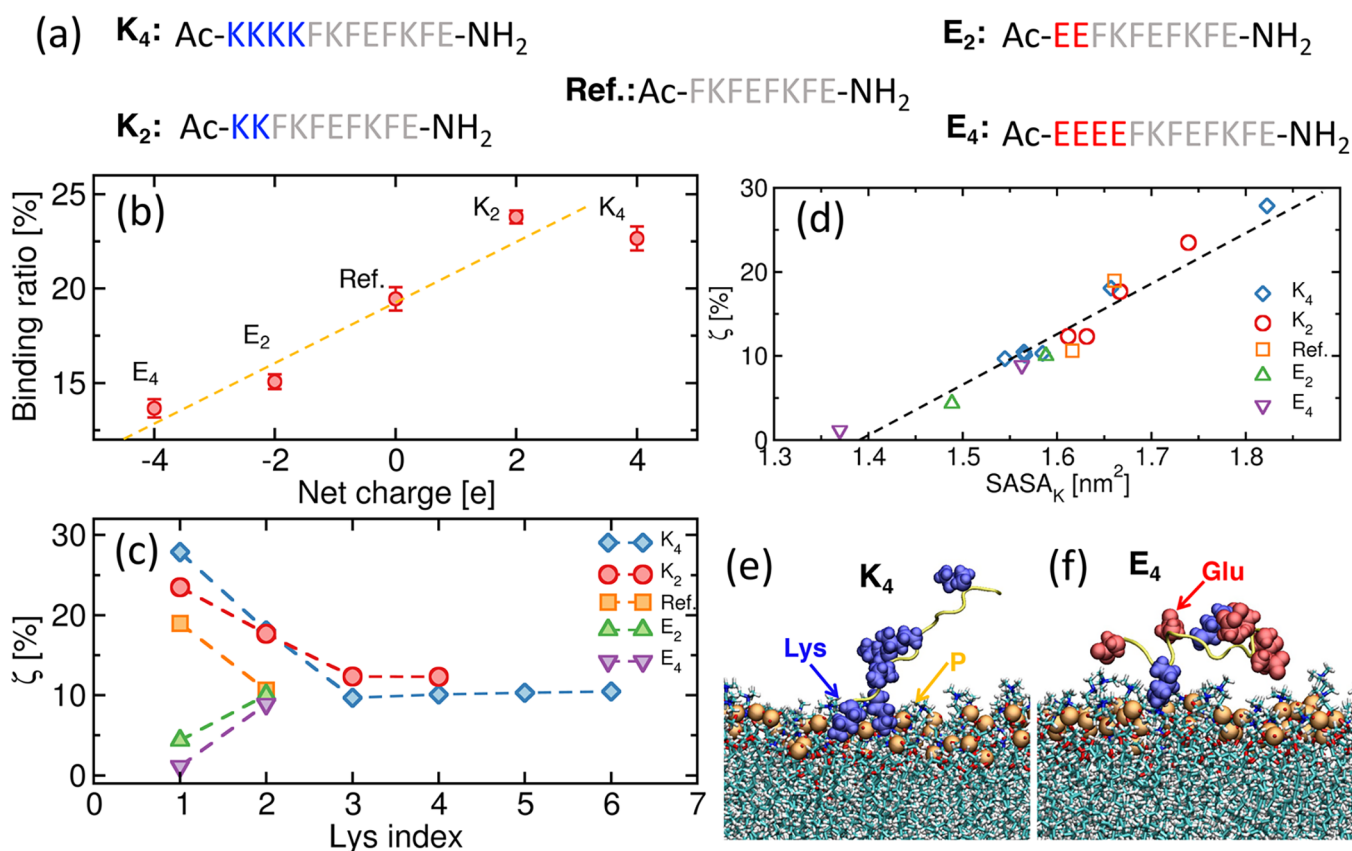
Figure 3. (a) Amino acid sequence of peptides K_4, K_2, reference, E_2, and E_4. (b) Binding ratios of peptides with respect to their net charge. (c) The percentage ζ of reversible-bound frames wherein the ith lysine is bound to a lipid. (d) The dependence of ζ on the $SASA_K$ for each lysine. Characteristic conformations of reversible-bound (e) K_4 and (f) E_4, wherein lysines are represented in blue, glutamic acids in red, and phosphate groups in orange.

by computing the standard deviation of the binding ratio for $(N - 1)$ trajectories where one of the N different simulations was removed each time during the calculation.

Net Peptide Charge. In order to study how the net charge of a peptide affects its binding to the membrane, two or four glutamic acid (E) or lysine (K) amino acids are added to the N-terminal of the neutral Ac-$(FKFE)_2$-NH_2 peptide to account for net charges of -4, -2, $+2$, and $+4$, respectively—see Figure 3a. These peptides are referred to as E_4, E_2, K_2, and K_4, respectively. It is important to notice that K and E amino acids differ also in the length of their side chain, which makes lysine moderately hydrophobic.

To compute binding ratios, five 1-μs trajectories were generated for E_4, E_2, and K_2 peptides. These peptides are mostly disordered in our simulations with all residues adopting coil structures consistently. In one of the simulations performed with the K_4 peptide, it formed a transient β-hairpin structure that survived for 0.2 μs. This suggests that the K_4 peptide can adopt more complex conformations and, therefore, requires more thorough sampling. We generated eight 1-μs simulations for this peptide such that its average binding ratio changed by only 0.3% when segments of the trajectories where it adopts β-hairpin conformations are removed from the analysis. Thus, for all peptides studied in this work, secondary structure formation is not a factor affecting peptide–membrane binding. The conformation of each peptide simulated here is characterized by its end-to-end distance in the Supporting Information—see Figures S18–S32. Note that, because of the finite size of the simulation box, the shortest

peptide (i.e., our reference peptide) can sample larger distances ξ from the membrane compared to E_4 and K_4 peptides. Binding ratios of the shortest peptides are, therefore, biased toward the unbound state compared to E_4 and K_4. To correct for this finite size effect, only frames for which $\xi < 2.5$ nm (where 2.5 nm is a distance sampled by all peptides) are taken into account when computing for binding ratios.

Figure 3b shows the binding ratios of peptides with a net charge varying from -4 to $+4$. This quantity increases monotonically with the net peptide charge up to $+2$. The binding ratio of K_4 is slightly lower than that for K_2 but still higher than that for the neutral reference peptide. This shows that positively charged peptides are more favorably attracted to lipid bilayers than neutral or negatively charged chains highlighting the importance of electrostatic interactions in this process. This trend is independent of our definition of binding ratio given by τ_{off}—see Figure S16. These results are consistent with previous studies on the reference peptide where negatively and positively charged side chains were shown to be repelled from and attracted to lipid membranes, respectively.[9]

Figure 3c characterizes contributions of each positive residue to membrane binding by computing the percentage ζ of reversible-bound frames in the trajectory wherein the ith lysine in the sequence is bound to a lipid. We consider that a lysine residue is bound to a lipid if the minimal atomic distance between these groups is less than 0.325 nm—see Figure 2c. The index i starts with the first lysine residue at the N-terminal. Figure 3c shows that, for K_4 and K_2, the two lysines close to
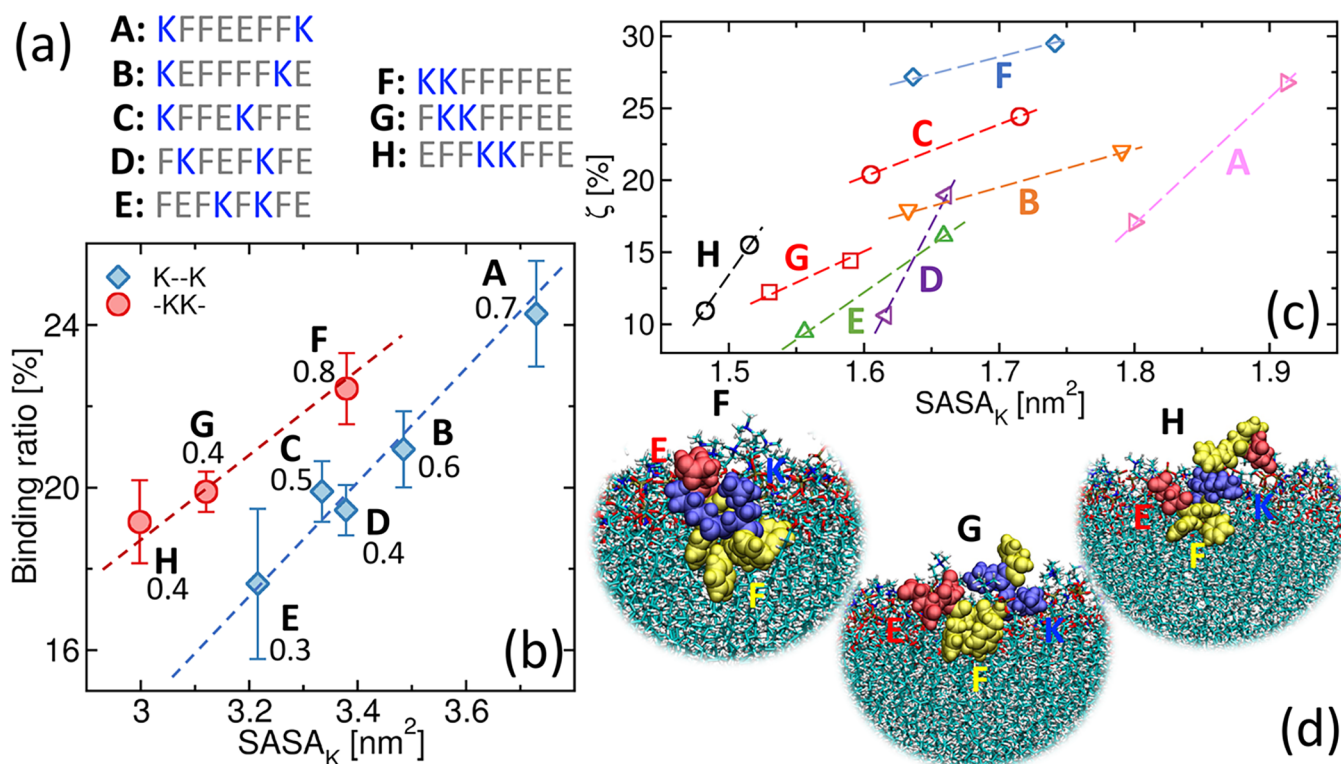
Figure 4. (a) Amino acid sequence of peptides A−H. (b) dependence of binding ratio on $SASA_K$ for peptides A−H. N_P for each peptide is shown as a number in (b). (c) dependence of ζ on the $SASA_K$ for each lysine. (d) Characteristic conformations of adsorbed peptides F, G, and H.

the N-terminal bind more frequently to lipids than the other positive residues defined by indices 3−6. For reference and anionic (i.e., E_2 and E_4) peptides, the first lysine in the sequence binds more and less frequently, respectively, than the second lysine.

To provide insight into the different contributions of lysine residues to membrane binding, Figure 3d shows the dependence of ζ on the solvent accessible surface area $SASA_K$ for each individual lysine. There is a clear positive correlation between these quantities, which shows that lysine residues that are more exposed to the solvent are also more likely to be attracted to the membrane. Since lysine residues that are located closer to one of the extremities of a peptide are expected to have a larger $SASA_K$, they are also expected to be more attracted to the membrane. This explains the larger ζ for the first lysine residues of K_4, K_2, and the reference peptide. The lower ζ of the first lysine residue in anionic peptides (green and purple symbols in Figure 3c) can be explained by its closer proximity to negative E side chains. These oppositely charged residues attract each other to form salt-bridges, which reduces $SASA_K$. Panels e and f show characteristic configurations of reversible-bound states for K_4 and E_4 peptides. In the former, lysine residues that are located closer to the N-terminal of the K_4 peptide are binding to negative phosphate atoms of the bilayer. In panel f, the lysine residue located closer to the N-terminal of the E_4 peptide is forming salt-bridges with negative glutamic acids and it is the second lysine that is binding to the membrane.

Peptide Sequence. In summary, Figure 3 shows that membrane binding is affected by both the net charge of a peptide and the position of its positive residues in the amino acid sequence. The latter affects the extent by which positive residues are exposed to the solvent and, therefore, can interact

with negative moieties of lipids. To better understand the relationship between exposure of positively charged residues and membrane binding, eight neutral sequences were designed by reordering the amino acids of the reference peptide. The two lysine residues are separated from each other by at least one residue for sequences A−E and placed consecutively in the amino acid sequence for peptides F−H—see Figure 4a. In these two sets of peptides, lysine residues are placed at different distances from the extremity of the peptide. The exposure of positive residues is quantified by computing the average solvent accessible surface area $SASA_K$ of both lysine residues over all reversible frames in which the peptide is not bound to the bilayer. This quantity varies from 2.99 to 3.73 nm^2, and it correlates with the position of lysine residues in the peptide sequence. In particular, sequences A, B, and F that have lysine residues located at the extremities of the peptide exhibit the largest $SASA_K$ in our simulations. Conversely, peptides that have lysine residues located in the middle of the sequence, e.g., peptides E and H, exhibit the lowest $SASA_K$ values—see Figure 4b.

The dependence of the binding ratio on $SASA_K$ is outlined in Figure 4b using red and blue dashed lines for peptides A−E and F−H, respectively. For these neutral sequences, the binding ratio increases with $SASA_K$ wherein peptides with the lowest and highest $SASA_K$ are found bound to the bilayer 15% and 25% of the time, respectively. Interestingly, these binding ratio levels are comparable to the ones for anionic (i.e., peptides E_2 and E_4) and cationic (K_2 and K_4) peptides in Figure 4b, respectively. Thus, adding positive residues to the N-terminal of a given peptide can have the same effect on membrane binding as increasing its $SASA_K$ by moving existing lysine residues to its extremities. Similarly, adding negative residues to the N-terminal can have the same effect as reducing

its $SASA_K$ by placing lysine residues in the middle of the peptide sequence.

In Figure 4b, peptides with the same $SASA_K$ have a higher binding ratio if their lysine residues are found consecutively in the peptide sequence (red dashed line in Figure 4b) as opposed to separated by other residues (blue line). This can be rationalized by noticing that both lysine residues are more likely to bind simultaneously to negative phosphate atoms of lipids if they are located close to each other as opposed to separated by several residues. This accounts for bound states that have a longer lifetime and, thus, a higher binding ratio. Evidence of increased lysine–phosphate binding for sequence F–H is provided by computing the number N_P of phosphate atoms bound to lysine residues. This quantity is shown as numbers in Figure 4b, which are computed by averaging over all frames in the reversible portions of the trajectories where the peptide is found bound to the membrane, i.e., $\xi < \xi_{cutoff}$. Peptide F binds to twice as many phosphate atoms as peptides D and C that have similar $SASA_K$. Similarly, peptide G has a higher N_P than peptide E.

Figure 4c depicts the percentage ζ of reversible-bound frames in which the first and second lysine residues are bound to the membrane. In particular, ζ is shown as a function of $SASA_K$ computed for each lysine residue for peptides A–H. This figure shows that lysine residues contribute more to the bound state if they have a large $SASA_K$. For example, lysine residues of peptides A, B, C, and F have a larger $SASA_K$ and ζ than peptides D, E, G, and H. However, this correlation is not as well-defined as that for charged peptides in Figure 3d, suggesting that other factors, e.g., other residues of the peptide, also play a role in accounting for bound states.

Out of the five 1-μs trajectories performed for each sequence (see Figures S6–S15), between 1 and 4 of them ended up with the peptide adsorbed onto the bilayer. Adsorbed states are stabilized by the burial of their non-polar residue in the dry bilayer core. This may involve the burial of four, three, or two phenylalanine residues as in the case of peptides F, G, and H in Figure 4d. A trend can be highlighted from an analysis of the trajectories in which peptides A–H are adsorbed. In particular, sequences D, E, and G, which have a phenylalanine residue at one extremity (i.e., the N-terminal), are found to be adsorbed in at least 60% of the trajectories—see Table 2. In contrast,

Table 2. Percentage of Trajectories in Which the Peptide Becomes Adsorbed onto the Membrane

	A	B	C	**D**	**E**	F	**G**	H
Adso. (%)	40	40	60	**60**	**80**	60	**60**	20

sequences A, B, C, F, and H with lysine or glutamic acid at their extremities are absorbed in 60% or less of the trajectories—see Table 2. This suggests that sequences that have phenylalaline residues at their extremities are more likely to be adsorbed onto the membrane. To test this ideas, five additional 1-μs simulations were performed with peptide Ac-FFKKFFEE-NH$_2$ which has two phenylalanine residues at the N-terminal. Figure 5a shows the minimal distance of this peptide in the different trajectories. The peptide becomes adsorbed to the membrane in less than 200 ns after only a few reversible binding events. The sequences of events leading to adsorption are shown in panels b and c for trajectory number 1. At 200 ns (panel b), only the first two phenylalanine residues are embedded into the membrane. At 700 ns (panel

c), all four phenylalanine residues become anchored into the membrane. This corroborates the trend observed for peptides A–G, but it needs to be validated with more trajectories and more peptide sequences.

Non-Polar Residues. The role played by non-polar residues in peptide–membrane binding is investigated by replacing phenylalanine residues of the reference peptide (i.e., **F**) with less hydrophobic valine (i.e., **V**) and alanine (i.e., **A**) amino acids. We will refer to these sequences as **F**-, **V**-, and **A**-peptides in this section. The binding ratio of these peptides computed from five 1-μs trajectories (as in previous sections) does not change significantly. It is 19% for both **F**- and **V**-peptides and 20% for the **A**-peptide. This corroborates the idea that the attraction of peptides to the lipid membranes, which accounts for reversible-bound states, is determined by charged residues and not non-polar amino acids. In contrast, the adsorbed state always involves the insertion of non-polar side chains into the hydrophobic interior of the lipid bilayer. Accordingly, in four out of the seven trajectories for the **F**-peptide (see Figure 2a), the peptide becomes adsorbed into the membrane. For the less hydrophobic peptides, adsorption only takes place in one of the five 1-μs trajectories of the **V**-peptide and in none of the trajectories for the **A**-peptide. Thus, more hydrophobic peptides become anchored into the membrane with a lesser probability to unbind from it.

■ CONCLUSION

In this paper, we explored effects of net charge, sequence pattern, and hydrophobicity on peptide–membrane binding using extensive all-atom molecular dynamics simulations. In a typical trajectory, the peptide that is initially located in the solvent undergoes several binding and unbinding events to the membrane before becoming adsorbed onto it. We show that the net charge of a peptide and the position of its charged residues in the sequence play an important role in accounting for the frequency of binding–unbinding events whereas non-polar residues affect peptide adsorption.

Our simulations are consistent with a previous study in which the presence of anionic lipids in the membrane increased the frequency of binding events, showing that charged moieties of the peptide are attracted to negative phosphate atoms of lipid membranes. Accordingly, we find that adding positive and negative residues to a peptide increases and decreases, respectively, its affinity to the membrane. Moreover, the frequency with which a peptide encounters the membrane is affected by the position of its positive residues in the peptide sequence. The latter affects the extent by which positive side chains are exposed to the solvent and, thus, can interact with the membrane. We find that positive residues at a peptide's extremity (i.e., N- and C-terminal) are more exposed to the solvent and, thus, encounter the membrane with a higher frequency. In contrast, positive residues located in the middle of the peptide sequence tend to be less exposed to the solvent and to bind the lipid bilayer with lesser frequency.

The adsorption of a peptide to the membrane involves burying its non-polar residues into the dry core of the lipid bilayer. Accordingly, we find that amphipathic peptides made using non-polar residues that have small (i.e., alanine and valine) and large (i.e., phenylalanine) transfer free energies from water to lipid bilayers[51] are adsorbed more and less frequently onto the membrane, respectively. In the same vein, we observe that the position of non-polar residues in the peptide sequence affects its tendency to be adsorbed onto the
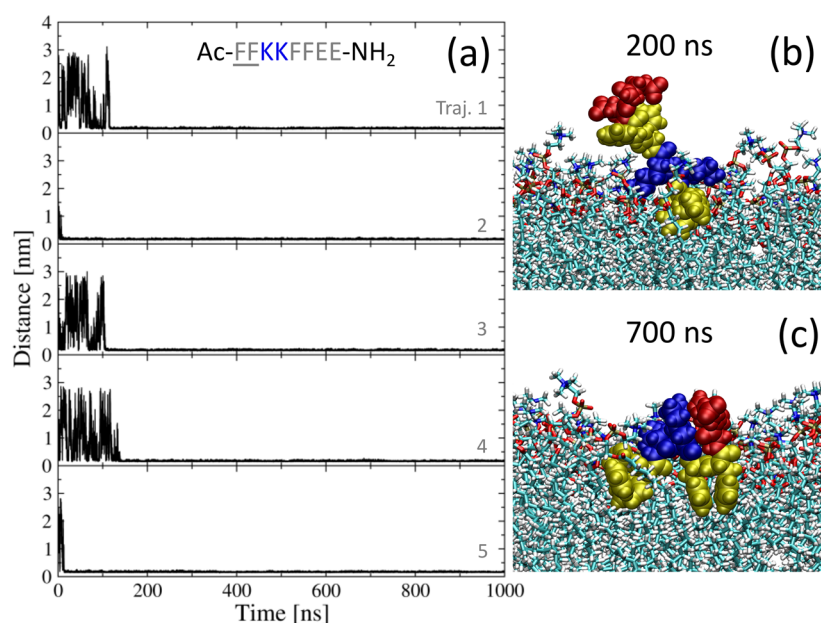
Figure 5. Minimal distance ξ between atoms of Ac-FFKKFFEE-NH$_2$ peptides and the bilayer in five independent trajectories. Characteristic conformations of adsorbed peptide at (b) 200 ns and (c) 700 ns for trajectory number 1.

membrane. Sequences with phenylalanine at the extremity of the peptide sequence have a higher tendency to be adsorbed in our simulations. The generality of this statement needs, however, to be further validated for other peptide sequences.

In summary, this current study provides insights into the mechanisms accounting for peptide–membrane binding and the role played by electrostatic and hydrophobic interactions in it. We anticipate that these insights will contribute to guide the design of new cell-penetrating peptides and more efficient antimicrobial peptides. Moreover, our results are consistent with previous studies in which electrostatic interactions between the peptide and the membrane were altered by either adding divalent cations to the solution[9,28] or tuning the lipid composition rendering the membrane charged.[9,30,52] The latter is intimately linked to the selectivity of certain peptides for cell membranes with specific lipid composition, which is important in designing efficient antimicrobial peptides with low toxicity to host cells.

ASSOCIATED CONTENT

Supporting Information

The Supporting Information is available free of charge at https://pubs.acs.org/doi/10.1021/acs.jpcb.2c06404.

> The minimal distance ξ for all the simulations in this study (section S1), the dependence of the binding ratio on τ_{off} (section S2), and the end-to-end distance of each peptide simulated (section S3) (PDF)

AUTHOR INFORMATION

Corresponding Author

Cristiano L. Dias − *Department of Physics, New Jersey Institute of Technology, Newark, New Jersey 07102-1982, United States;* ⦿ orcid.org/0000-0002-8765-3922; Email: cld@njit.edu

Author

Yanxing Yang − *Department of Physics, New Jersey Institute of Technology, Newark, New Jersey 07102-1982, United States;* ⦿ orcid.org/0000-0003-2521-6441

Complete contact information is available at:
https://pubs.acs.org/10.1021/acs.jpcb.2c06404

Notes

The authors declare no competing financial interest.

REFERENCES

(1) Owen, M. C.; Gnutt, D.; Gao, M.; Wärmländer, S. K.; Jarvet, J.; Gräslund, A.; Winter, R.; Ebbinghaus, S.; Strodel, B. Effects of in vivo conditions on amyloid aggregation. *Chem. Soc. Rev.* **2019**, *48*, 3946–3996.

(2) Cecchi, C.; Baglioni, S.; Fiorillo, C.; Pensalfini, A.; Liguri, G.; Nosi, D.; Rigacci, S.; Bucciantini, M.; Stefani, M. Insights into the molecular basis of the differing susceptibility of varying cell types to the toxicity of amyloid aggregates. *J. Cell Sci.* **2005**, *118*, 3459–3470.

(3) Julien, C.; Tomberlin, C.; Roberts, C. M.; Akram, A.; Stein, G. H.; Silverman, M. A.; Link, C. D. In vivo induction of membrane damage by β-amyloid peptide oligomers. *Acta Neuropathol. Commun.* **2018**, *6*, 131.

(4) Zasloff, M. Antimicrobial peptides of multicellular organisms. *Nature* **2002**, *415*, 389–395.

(5) Magana, M.; Pushpanathan, M.; Santos, A. L.; Leanse, L.; Fernandez, M.; Ioannidis, A.; Giulianotti, M. A.; Apidianakis, Y.; Bradfute, S.; Ferguson, A. L.; et al. The value of antimicrobial peptides in the age of resistance. *Lancet Infect. Dis.* **2020**, *20*, e216−e230.

(6) Fjell, C. D.; Hiss, J. A.; Hancock, R. E.; Schneider, G. Designing antimicrobial peptides: form follows function. *Nat. Rev. Drug Discovery* **2012**, *11*, 37−51.

(7) López de la Paz, M.; Goldie, K.; Zurdo, J.; Lacroix, E.; Dobson, C. M.; Hoenger, A.; Serrano, L. De novo designed peptide-based amyloid fibrils. *Proc. Natl. Acad. Sci. U. S. A.* **2002**, *99*, 16052−16057.

(8) Tjernberg, L.; Hosia, W.; Bark, N.; Thyberg, J.; Johansson, J. Charge Attraction and β Propensity Are Necessary for Amyloid Fibril Formation from Tetrapeptides. *J. Biol. Chem.* **2002**, *277*, 43243−43246.

(9) Yang, Y.; Jalali, S.; Nilsson, B. L.; Dias, C. L. Binding mechanisms of amyloid-like peptides to lipid bilayers and effects of divalent cations. *ACS Chem. Neurosci.* **2021**, *12*, 2027−2035.

(10) Yang, Y.; Distaffen, H.; Jalali, S.; Nieuwkoop, A. J.; Nilsson, B. L.; Dias, C. L. Atomic Insights into Amyloid-Induced Membrane Damage. *ACS Chem. Neurosci.* **2022**, *13*, 2766−2777.

(11) Park, P.; Franco, L. R.; Chaimovich, H.; Coutinho, K.; Cuccovia, I. M.; Lima, F. S. Binding and flip as initial steps for BP-100 antimicrobial actions. *Sci. Rep.* **2019**, *9*, 8622.

(12) Ciudad, S.; Puig, E.; Botzanowski, T.; Meigooni, M.; Arango, A. S.; Do, J.; Mayzel, M.; Bayoumi, M.; Chaignepain, S.; Maglia, G.; et al. Aβ (1−42) tetramer and octamer structures reveal edge conductivity pores as a mechanism for membrane damage. *Nat. Commun.* **2020**, *11*, 3014.

(13) Hane, F.; Drolle, E.; Gaikwad, R.; Faught, E.; Leonenko, Z. Amyloid-beta aggregation on model lipid membranes: an atomic force microscopy study. *J. Alzheimers Dis.* **2011**, *26*, 485−494.

(14) Drolle, E.; Gaikwad, R. M.; Leonenko, Z. Nanoscale electrostatic domains in cholesterol-laden lipid membranes create a target for amyloid binding. *Biophys. J.* **2012**, *103*, L27−L29.

(15) Hellstrand, E.; Sparr, E.; Linse, S. Retardation of Abeta fibril formation by phospholipid vesicles depends on membrane phase behavior. *Biophys. J.* **2010**, *98*, 2206−2214.

(16) Bonev, B.; Watts, A.; Bokvist, M.; Gröbner, G. Electrostatic peptide−lipid interactions of amyloid-beta peptide and pentalysine with membrane surfaces monitored by 31P MAS NMR. *Phys. Chem. Chem. Phys.* **2001**, *3*, 2904−2910.

(17) Moores, B.; Drolle, E.; Attwood, S. J.; Simons, J.; Leonenko, Z. Effect of surfaces on amyloid fibril formation. *PLoS One* **2011**, *6*, No. e25954.

(18) Zhang, X.; St. Clair, J. R.; London, E.; Raleigh, D. P. Islet amyloid polypeptide membrane interactions: effects of membrane composition. *Biochemistry (Mosc.)* **2017**, *56*, 376−390.

(19) Chi, E. Y.; Ege, C.; Winans, A.; Majewski, J.; Wu, G.; Kjaer, K.; Lee, K. Y. C. Lipid membrane templates the ordering and induces the fibrillogenesis of Alzheimer's disease amyloid-β peptide. *Proteins: Struct., Funct., Bioinf.* **2008**, *72*, 1−24.

(20) Yu, X.; Wang, Q.; Pan, Q.; Zhou, F.; Zheng, J. Molecular interactions of Alzheimer amyloid-β oligomers with neutral and negatively charged lipid bilayers. *Phys. Chem. Chem. Phys.* **2013**, *15*, 8878.

(21) Jiang, Z.; Vasil, A. I.; Hale, J. D.; Hancock, R. E. W.; Vasil, M. L.; Hodges, R. S. Effects of net charge and the number of positively charged residues on the biological activity of amphipathic α-helical cationic antimicrobial peptides. *Biopolymers* **2008**, *90*, 369−383.

(22) Lopez Cascales, J. J.; Zenak, S.; Garcia de la Torre, J.; Lezama, O. G.; Garro, A.; Enriz, R. D. Small cationic peptides: Influence of charge on their antimicrobial activity. *ACS Omega* **2018**, *3*, 5390−5398.

(23) Yin, L. M.; Edwards, M. A.; Li, J.; Yip, C. M.; Deber, C. M. Roles of hydrophobicity and charge distribution of cationic antimicrobial peptides in peptide-membrane interactions. *J. Biol. Chem.* **2012**, *287*, 7738−7745.

(24) Ringstad, L.; Schmidtchen, A.; Malmsten, M. Effect of peptide length on the interaction between consensus peptides and DOPC/ DOPA bilayers. *Langmuir* **2006**, *22*, 5042−5050.

(25) Javanainen, M.; Melcrová, A.; Magarkar, A.; Jurkiewicz, P.; Hof, M.; Jungwirth, P.; Martinez-Seara, H. Two cations, two mechanisms: interactions of sodium and calcium with zwitterionic lipid membranes. *Chem. Commun.* **2017**, *53*, 5380−5383.

(26) Catte, A.; Girych, M.; Javanainen, M.; Loison, C.; Melcr, J.; Miettinen, M. S.; Monticelli, L.; Määttä, J.; Oganesyan, V. S.; Ollila, O. H. S.; et al. Molecular electrometer and binding of cations to phospholipid bilayers. *Phys. Chem. Chem. Phys.* **2016**, *18*, 32560−32569.

(27) Nguyen, M. T. H.; Biriukov, D.; Tempra, C.; Baxova, K.; Martinez-Seara, H.; Evci, H.; Singh, V.; Šachl, R.; Hof, M.; Jungwirth, P.; Javanainen, M.; Vazdar, M. Ionic strength and solution composition dictate the adsorption of cell-penetrating peptides onto phosphatidylcholine membranes. *Langmuir* **2022**, *38*, 11284−11295.

(28) Sciacca, M. F.; Milardi, D.; Messina, G. M.; Marletta, G.; Brender, J. R.; Ramamoorthy, A.; Rosa, C. L. Cations as switches of amyloid-mediated membrane disruption mechanisms: calcium and IAPP. *Biophys. J.* **2013**, *104*, 173−184.

(29) Sciacca, M. F.; Kotler, S. A.; Brender, J. R.; Chen, J.; Lee, D.-k.; Ramamoorthy, A. Two-step mechanism of membrane disruption by A-β through membrane fragmentation and pore formation. *Biophys. J.* **2012**, *103*, 702−710.

(30) Sciacca, M. F. M.; Monaco, I.; La Rosa, C.; Milardi, D. The active role of Ca^{2+} ions in Aβ-mediated membrane damage. *Chem. Commun.* **2018**, *54*, 3629−3631.

(31) Huang, Y.; Huang, J.; Chen, Y. Alpha-helical cationic antimicrobial peptides: relationships of structure and function. *Protein & Cell* **2010**, *1*, 143−152.

(32) Lee, D. G.; Kim, H. N.; Park, Y.; Kim, H. K.; Choi, B. H.; Choi, C.-H.; Hahm, K.-S. Design of novel analogue peptides with potent antibiotic activity based on the antimicrobial peptide, HP (2−20), derived from N-terminus of Helicobacter pylori ribosomal protein L1. *Biochim. Biophys. Acta* **2002**, *1598*, 185−194.

(33) Chen, L.; Harrison, S. Cell-penetrating peptides in drug development: enabling intracellular targets. *Biochem. Soc. Trans.* **2007**, *35*, 821−825.

(34) Kustanovich, I.; Shalev, D. E.; Mikhlin, M.; Gaidukov, L.; Mor, A. Structural requirements for potent censure selective cytotoxicity for antimicrobial dermaseptin S4 derivatives. *J. Biol. Chem.* **2002**, *277*, 16941−16951.

(35) Zelezetsky, I.; Pacor, S.; Pag, U.; Papo, N.; Shai, Y.; Sahl, H.-G.; Tossi, A. Controlled alteration of the shape and conformational stability of α-helical cell-lytic peptides: effect on mode of action and cell specificity. *Biochem. J.* **2005**, *390*, 177−188.

(36) Dathe, M.; Wieprecht, T.; Nikolenko, H.; Handel, L.; Maloy, W.; MacDonald, D. L.; Beyermann, M.; Bienert, M. Hydrophobicity, hydrophobic moment and angle subtended by charged residues modulate antibacterial and haemolytic activity of amphipathic helical peptides. *FEBS Lett.* **1997**, *403*, 208−212.

(37) Lockhart, C.; Klimov, D. K. Calcium enhances binding of Aβ monomer to DMPC lipid bilayer. *Biophys. J.* **2015**, *108*, 1807−1818.

(38) Zhao, T.; Liu, X.; Singh, S.; Liu, X.; Zhang, Y.; Sawada, J.; Komatsu, M.; Belfield, K. D. Mitochondria penetrating peptide-conjugated TAMRA for live-cell long-term tracking. *Bioconjugate Chem.* **2019**, *30*, 2312−2316.

(39) Bowerman, C. J.; Nilsson, B. L. A reductive trigger for peptide self-assembly and hydrogelation. *J. Am. Chem. Soc.* **2010**, *132*, 9526−9527.

(40) Marini, D. M.; Hwang, W.; Lauffenburger, D. A.; Zhang, S.; Kamm, R. D. Left-handed helical ribbon intermediates in the self-assembly of a β-sheet peptide. *Nano Lett.* **2002**, *2*, 295−299.

(41) Jalali, S.; Yang, Y.; Mahmoudinobar, F.; Singh, S. M.; Nilsson, B. L.; Dias, C. Using all-atom simulations in explicit solvent to study aggregation of amphipathic peptides into amyloid-like fibrils. *J. Mol. Liq.* **2022**, *347*, 118283.

(42) Lee, J.; Cheng, X.; Swails, J. M.; Yeom, M. S.; Eastman, P. K.; Lemkul, J. A.; Wei, S.; Buckner, J.; Jeong, J. C.; Qi, Y.; et al. CHARMM-GUI input generator for NAMD, GROMACS, AMBER, OpenMM, and CHARMM/OpenMM simulations using the CHARMM36 additive force field. *J. Chem. Theory Comput.* **2016**, *12*, 405−413.

(43) Jo, S.; Lim, J. B.; Klauda, J. B.; Im, W. CHARMM-GUI membrane builder for mixed bilayers and its application to yeast membranes. *Biophys. J.* **2009**, *97*, 50−58.

(44) Jo, S.; Kim, T.; Iyer, V. G.; Im, W. CHARMM-GUI: a web-based graphical user interface for CHARMM. *J. Comput. Chem.* **2008**, *29*, 1859−1865.

(45) Abraham, M. J.; Murtola, T.; Schulz, R.; Páll, S.; Smith, J. C.; Hess, B.; Lindahl, E. GROMACS: High performance molecular simulations through multi-level parallelism from laptops to super-computers. *SoftwareX* **2015**, *1−2*, 19−25.

(46) Klauda, J. B.; Venable, R. M.; Freites, J. A.; O'Connor, J. W.; Tobias, D. J.; Mondragon-Ramirez, C.; Vorobyov, I.; MacKerell, A. D.; Pastor, R. W. Update of the CHARMM all-atom additive force field for lipids: validation on six lipid types. *J. Phys. Chem. B* **2010**, *114*, 7830−7843.

(47) Nosé, S. A unified formulation of the constant temperature molecular dynamics methods. *J. Chem. Phys.* **1984**, *81*, 511−519.

(48) Hoover, W. G. Canonical dynamics: Equilibrium phase-space distributions. *Phys. Rev. A* **1985**, *31*, 1695−1697.

(49) Parrinello, M.; Rahman, A. Polymorphic transitions in single crystals: a new molecular dynamics method. *J. Appl. Phys.* **1981**, *52*, 7182−7190.

(50) Darden, T.; York, D.; Pedersen, L. Particle mesh Ewald: an Nlog(N) method for Ewald sums in large systems. *J. Chem. Phys.* **1993**, *98*, 10089−10092.

(51) Wimley, W. C.; White, S. H. Experimentally determined hydrophobicity scale for proteins at membrane interfaces. *Nat. Struct. Mol. Biol.* **1996**, *3*, 842−848.

(52) Dias, C. L.; Jalali, S.; Yang, Y.; Cruz, L. Role of Cholesterol on Binding of Amyloid Fibrils to Lipid Bilayers. *J. Phys. Chem. B* **2020**, *124*, 3036.